

Charge and current fluctuations in a superconducting single electron transistor near a Cooper pair resonance

Mahn-Soo Choi

Korea Institute for Advanced Study, Cheongryanri-dong 207-43, Seoul 130-012, Korea

Francesco Plastina and Rosario Fazio

NEST-INFM & Scuola Normale Superiore, I-56127 Pisa, Italy

cond-mat/0208165

(Dated: October 30, 2018)

We analyze charge tunneling statistics and current noise in a superconducting single-electron transistor in a regime where the Josephson-quasiparticle cycle is the dominant mechanism of transport. Due to the interplay between Coulomb blockade and Josephson coherence, the probability distribution for tunneling events strongly deviates from a Poissonian and displays a pronounced even-odd asymmetry in the number of transmitted charges. The interplay between charging and coherence is reflected also in the zero-frequency current noise which is significantly quenched when the quasi-particle tunneling rates are comparable to the coherent Cooper-pair oscillation frequency. Furthermore the finite frequency spectrum shows a strong enhancement near the resonant transition frequency for Josephson tunneling.

PACS numbers: 72.70.+m, 73.23Hk, 74.50+r

I. INTRODUCTION

Shot noise in a mesoscopic conductor is a consequence of the stochastic character of electron tunneling and of the discreteness of charge. Unlike thermal noise, shot noise describes the non-equilibrium fluctuations of current; therefore, the study of current fluctuations can provide further understanding of properties related to correlation mechanisms, internal energy scales or the carrier statistics which cannot be obtained by measuring the average current^{1,2,3,4}.

A well studied example of physical processes where electron correlations play a dominant role is the phenomenon of Coulomb blockade. In a system of small tunneling junctions, due to the large electrostatic energy (as compared to temperature or voltages), the electronic charge is transported one by one. This effect leads to many remarkable features in transport properties and has been a subject of extensive study for the last decades^{5,6}. As an example, the strong dependence of the current-voltage characteristics on the gate charge was exploited to use a single electron transistor (SET) as a highly sensitive charge detector⁷, and proposed as measuring apparatus of the charge state of a Josephson quantum bit^{8,9,10,11}. Since it leads to a strong correlation of consecutive tunneling events, Coulomb blockade has turned out to manifest itself in a peculiar way on the current noise. Such an effect has been studied both in the sequential tunneling^{3,4,12,13} and in the cotunneling regime^{14,15}. Additional interest in studying noise in single electron devices comes from the recently proposed schemes that employ current fluctuation measurements to detect entanglement in solid state systems¹⁶.

An even richer scenario occurs when the coherence of charge carriers is maintained over a significant portions

of the system. Such a circumstance is encountered quite often when the tunneling junctions are superconducting. In this case, the charge carriers are Cooper pairs, and their coherent tunneling across the junctions gives rise to a series of pronounced structures in the *I-V* characteristics at sub-gap voltages^{17,18,19}. Furthermore, as analyzed in Ref. 20, the scattering of quasi-particles (and consequently the shot noise) in superconducting point contacts is significantly enhanced in the presence of the supercurrent produced by a coherent flow of Cooper pairs.

In this paper, we analyze a superconducting double tunnel junction device, operating in a suitably chosen bias voltage regime, such that one of the junctions of the SET is on resonance for Cooper pair tunneling (the case where Cooper pair resonance occurs on both junctions has been recently analyzed in Ref. 21). The interplay between coherence and interaction is explored by sweeping the operating point of the device through the Cooper pair resonance. We will show that the fluctuations of the charge on the central island are sensitive to both Coulomb blockade and quantum coherence. More pronounced effects arise in the regime in which the rates of incoherent quasi-particle tunneling matches the frequency of coherent Cooper-pair oscillation. This gives rise to an enhanced fluctuation of charge in the central-island and to a substantial suppression of the current noise. By investigating the statistics of the tunneling events, we show that the suppression in the shot noise is related to the deviation of the counting statistics from the Poissonian distribution. The probability distribution of tunneling events exhibits a parity dependence and remains non-Poissonian in a wide range of parameter values. The interplay between coherence and Coulomb blockade affects the overall charge transport and is also clearly observed in the finite frequency behavior of the

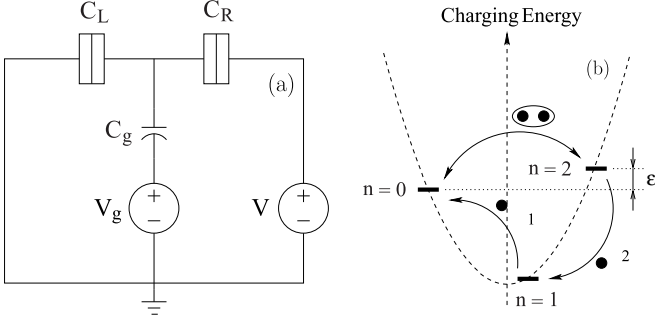


FIG. 1: Schematic diagrams of (a) the superconducting SET device and (b) the transition processes between relevant charge states.

current noise. Its power spectrum displays a sharp resonance peak at the Josephson frequency, resulting from coherent oscillations between two quantum states.

The work presented here applies to the setup used in a recent experiment²² to probe the coherent evolution of quantum states in a Cooper pair box as well as in an earlier experiment¹⁷ on resonant Cooper pair tunneling. In this paper we extend the results of Ref. 23. The paper is organized as follows. In Section II, we introduce the model to describe the SET transistor and we describe the relevant processes involved in the Josephson-quasiparticle cycle. In the same section we also introduce the master equation, in its general form, used to obtain all the results of this work. The solution of the master equation is worked out to analyze in detail the fluctuations of the charge on the central electrode and, in particular, the spectrum of the charge fluctuation as measured by a detector coupled to the island (Section III), the counting statistics for the tunneled charges (Section IV), and the shot noise of the current (Section V). In Section V we discuss in some details the properties of the shot noise at zero frequency, making explicit the results already contained in the counting statistics. In the same section we also discuss the frequency dependence of the shot noise. Section VI is devoted to the conclusions.

II. THE MODEL

The system we consider is a superconducting SET (see Fig. 1), which consists in a small central electrode (island) connected by tunnel junctions to two leads and capacitively coupled to a gate electrode. The electrostatic energy of the island can be adjusted by controlling the gate voltage V_g . A transport voltage V is applied to the outer leads, determining the current flowing through the device. Letting C_g , C_L and C_R be the gate and left and right junction capacitances, respectively, the electrostatic charging energy is given by $E_C = e^2/2C_\Sigma$ where $C_\Sigma = C_g + C_L + C_R$ is the total capacitance of the island. The device operates in the Coulomb blockade regime, i.e. with the charging energy much larger than

both the Josephson coupling energy E_J and the thermal energy $k_B T$ ($E_C \gg E_J, k_B T$), but still much smaller than the superconducting gap Δ which we suppose to be the largest energy scale in the problem. Charge can pass through the tunnel barriers coherently and incoherently. In addition to quasi-particle tunneling, Josephson effect allows to maintain coherence in the Cooper-pair tunneling processes. This coherence does play an important role in transport as long as charge states which differ by one Cooper pair are almost degenerate. The Hamiltonian of the system is given by

$$H_{\text{tot}} = H_L + H_R + H_I + H_T + H_C \quad (1)$$

where H_α ($\alpha = L, R, I$) is the BCS Hamiltonian of the left (L), right (R) lead and of the central island (I). The tunneling Hamiltonian²⁴ is

$$H_T = \sum_{j=L,R} \sum_{kq\sigma} \left[T_{kq} e^{-i\phi_j} c_{kq\sigma}^\dagger c_{qI\sigma} + h.c. \right], \quad (2)$$

where T_{kq} is the tunneling amplitude and $c_{k\alpha}^\dagger$ ($c_{k\alpha}$) creates (annihilates) a particle with momentum k and energy $\varepsilon_{k\alpha}$ in electrode α . The variable $\phi_{L,R}$ is the superconducting phase difference at the left (right) junction and it is canonically conjugated to the number $n_{L,R}$ of electrons that have passed across the left (right) junction *out of* the central electrode ($[n_k, \phi_j] = i\delta_{jk}$). Finally, H_C is the electrostatic energy,

$$H_C = E_C(n + n_0)^2 + eVn_R, \quad (3)$$

where $n = -n_L - n_R$ is the number of excess electrons on the central island, while $en_0 \equiv C_R V + C_g V_g$ is the offset charge due to the applied voltages.

For later convenience it is useful to define the part of the Hamiltonian which accounts for the coherent dynamics of the macroscopic variable n . It includes the charging and the Josephson terms. By properly adjusting the bias and gate voltages, one can put either the right or left junction at such a resonance for Cooper-pair tunneling. We consider the case of resonance across the left junction, and consequently we keep only the corresponding Josephson coupling

$$H_0 = E_C(n + n_0)^2 + eVn_R - E_J \cos(2\phi_L). \quad (4)$$

A quasi-particle tunneling *into* (*out of*) the island across the junctions leads to the transition $n \rightarrow n + 1$ ($n \rightarrow n - 1$) of the island charge. The rates of these incoherent processes are given by the relation

$$\Gamma_{L/R}^\pm(n) = \left[\coth(\beta \mathcal{E}_{n,\pm}^{L/R}) \pm 1 \right] \frac{\text{Im} I_{\text{qp}}(\mathcal{E}_{n,\pm}^{L/R})}{2e}, \quad (5)$$

where $\mathcal{E}_{n,\pm}^L = \pm E_{n,n\pm 1}$, $\mathcal{E}_{n,\pm}^R = eV \pm E_{n,n\pm 1}$, $E_{m,n} = E_C(m-n)(m+n+2n_0)$, and $I_{\text{qp}}(E)$ is the quasi-particle tunneling current at the bias voltage E/e in the absence of charging effects (see, e.g., Ref. 25 for an explicit expression of I_{qp} in terms of T_{kq}).

Since the SET transistor operates in the charge regime ($E_C \gg E_J$), we can take advantage of the strong suppression of charge fluctuations to use the eigenstates of n as basis states for the island. Moreover, we focus on the bias regime $|eV| \simeq 2\Delta + E_C$ where only the two charge states with $n = 0$ and $n = 2$, are nearly degenerate. Such a condition implies that quasi-particle tunneling only takes place from the central island toward the right electrode, while the left junction allows only for coherent Cooper pair tunneling. Furthermore, we suppose that the Josephson energy of the right junction is negligible (the corresponding term has already been omitted from H_0 , which is justified within the rotating wave approximation). All these conditions are met in the recent experiment by Nakamura *et al.*²², designed to probe the state of the island via the detection of the incoherent tunneling current. In this situation one can imagine that the coherent Cooper-pair tunneling occurring across the left junction is interrupted from time to time by quasi-particle tunneling across the right junction, as sketched in Fig.1 (b).

Due to the strong Coulomb blockade, it suffices to keep the three charge states, $n = 0, 1, 2$, and two tunneling rates, $\Gamma_1 \equiv \Gamma_R^-(1)$ and $\Gamma_2 \equiv \Gamma_R^-(2)$; the other tunneling

rates are exponentially suppressed. In order to simplify the notation, we assume that $\Gamma_1 = \Gamma_2 \equiv \Gamma$, which is a very good approximation in the regime we are interested in. For example, in the experiment of Ref. 22, $1/\Gamma_1 = 8\text{ns}$ and $1/\Gamma_2 = 6\text{ns}$.

The transport properties of the system in the set-up described above can be well described in terms of two variables, either n and n_L or n and n_R ($n = -n_L - n_R$). However, the quantum dynamics of these system is affected by the quantum noise due to the coupling to the environment provided by the fermionic bath. In order to describe this effect, we adopt a master equation approach, which has been widely used to describe quantum open systems²⁶. A master equation for the reduced density matrix $\rho(t) = \text{Tr}_{qp} \rho_{\text{tot}}(t)$ is obtained by taking the trace over the fermionic degrees of freedom from the Liouville equation ($\hbar = 1$)

$$\partial_t \rho_{\text{tot}}(t) = -i [H_{\text{tot}}, \rho_{\text{tot}}(t)] \quad (6)$$

for the density matrix ρ_{tot} of the system plus environment. The resulting equation can then be written in the Lindblad form as^{18,19,23,26,27}

$$\partial_t \rho(t) = -i [H_0, \rho(t)] + \frac{1}{2} \sum_{n=1,2} \Gamma_n \left[2L_n \rho(t) L_n^\dagger - L_n^\dagger L_n \rho(t) - \rho(t) L_n^\dagger L_n \right]. \quad (7)$$

Here L_n is a Lindblad operator corresponding to the quantum jump $n \rightarrow n-1$ and $n_R \rightarrow n_R+1$, i.e., in the $|n, n_R\rangle$ -basis $L_n = |n-1, n_R+1\rangle \langle n, n_R|$. The first term describes a purely phase-coherent dynamics, while the second one is responsible for both dephasing and relaxation due to the quasi-particle tunneling.

The solution of the Eq. (7) behaves in distinct ways in the two limiting cases of strong and weak coupling with the quasi-particle reservoir. In the *strong dephasing limit* (either $\Gamma \gg E_J$ or $\varepsilon \gg E_J$, see below), the dephasing time τ_φ , which describes the decay of the off-diagonal elements of ρ to their stationary values, is small compared to the relaxation time τ_r which sets the time-scale for the variation of the diagonal elements (i.e. population of the charge states). The relaxation time is given by

$$\frac{1}{\tau_r} = \Gamma_r = \frac{2E_J^2 \Gamma}{4\varepsilon^2 + \Gamma^2}. \quad (8)$$

On the other hand, in the *weak dephasing limit* ($\Gamma, \varepsilon \ll E_J$), there is no such a clear separation of time scales; both the diagonal and off-diagonal elements vary over the same time scale $1/\Gamma$.

III. FLUCTUATIONS OF THE CHARGE ON THE ISLAND

A first insight into the interplay among coherent Cooper-pair tunneling, Coulomb blockade, and incoherent quasi-particle tunneling can be obtained by examining the fluctuations of the charges on the island as a function of the quasi-particle tunneling rate Γ , the gate voltage, and the Josephson coupling energy. In this case, we only need to keep track of the variable n , and thus define a reduced density matrix for the central island charge, $\sigma(t) = \text{Tr}_{n_R} \rho(t)$, which satisfies an equation identical to Eq. (7), but with $L_n = |n-1\rangle \langle n|$ now operating on the reduced ' n ' space only²⁷. In the stationary state, the master equation has the solution ($\sigma_{mn} = \langle m | \sigma | n \rangle$)

$$\sigma_{00} = \frac{1 + (4\varepsilon^2 + \Gamma^2)/E_J^2}{3 + (4\varepsilon^2 + \Gamma^2)/E_J^2} \quad (9a)$$

$$\sigma_{11} = \sigma_{22} = \frac{1}{3 + (4\varepsilon^2 + \Gamma^2)/E_J^2} \quad (9b)$$

$$\sigma_{02} = \sigma_{20}^* = -i \frac{E_J(\sigma_{00} - \sigma_{22})}{\Gamma + 2i\varepsilon} \quad (9c)$$

Here $\varepsilon = 4E_C(1 + n_0)$ measures the energy difference between the state with $n = 0$ and $n = 2$ charge on the

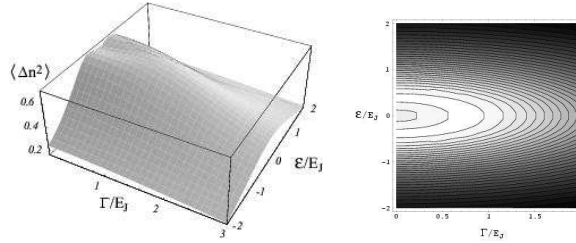


FIG. 2: Variance $\langle(\Delta n)^2\rangle$ of the charge on the island as a function of $\Gamma_1 = \Gamma_2 = \Gamma$ and ε .

island; the Cooper pair resonance corresponds to $\varepsilon = 0$.

From the stationary-state solution (9), we evaluate the characteristic function $C(\theta) = \langle e^{-in\theta} \rangle$ for the quantum variable n . It is given by

$$C(\theta) = \frac{E_J^2(e^{-2i\theta} + e^{-i\theta} + 1) + 4\varepsilon^2 + \Gamma^2}{4\varepsilon^2 + \Gamma^2 + 3E_J^2} \quad (10)$$

From $C(\theta)$ one can evaluate all the statistical moments of the charge on the island; in particular, we concentrate on the variance

$$\langle(\Delta n)^2\rangle = E_J^2 \frac{5(4\varepsilon^2 + \Gamma^2) + 6E_J^2}{[4\varepsilon^2 + \Gamma^2 + 3E_J^2]^2} \quad (11)$$

shown in Fig. 2.

An interesting point about the result in Eq. (11) is that the maximum of the variance is found at $\Gamma_{\text{opt}} \simeq \sqrt{3/5} E_J$ for $\varepsilon = 0$. In other words, the fluctuation is enhanced when the decoherence time matches the time for the Josephson coherent oscillations. Moreover as $|\varepsilon|$ increases (up to $|\varepsilon| < E_J \sqrt{3/20}$), the optimal value of Γ decreases as $\Gamma_{\text{opt}} \simeq \sqrt{3E_J^2/5 - 4\varepsilon^2}$; meaning that ε enhances the effective dephasing rates. These two features will appear more clearly when we discuss the statistics (Section IV) and noise (Section V) of the transport across the junctions.

An important quantity to consider is the fluctuation spectrum for the number of electron charge residing on the island. As already discussed by many authors, it is important to include the back-action of the measuring apparatus^{8,9,10}, which could be a SET transistor capacitively coupled to the central island. We include the charge detector coupling via an Hamiltonian term of the form

$$\delta H_{\text{det}} = -\hat{n} D$$

where D is a detector operator. Assuming the correlation time for the detector to be the fastest time scale of the problem, we write (here we follow Averin's treatment¹⁰):

$$\langle D(t + \tau) D(t) \rangle = \gamma_d \delta(\tau). \quad (12)$$

The non-zero value of γ_d is the essential cause of the measurement back-action. Indeed, a term proportional

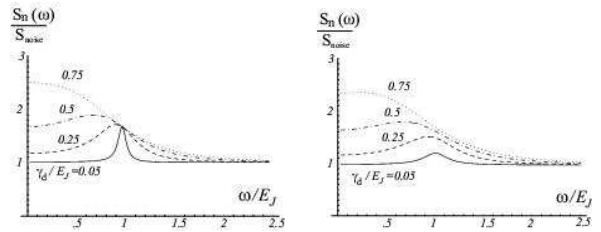


FIG. 3: Charge fluctuation spectrum in the weak dephasing regime at degeneracy ($\varepsilon = 0$), with the indicated back-action rate values and with $\Gamma/E_J = 10^{-5}$ (left) and $\Gamma/E_J = 0.1$ (right).

to γ_d enters the master equation Eq.(7), thus affecting the time evolution of the system variables. To effectively measure the charge number, we look at an output detector operator O , which, in the linear regime, evolves as $O(t) = O^{(0)} + \lambda \hat{n}(t)$, (see Ref.10). The response coefficient λ is determined by the imaginary part of the equilibrium correlation function $\langle O(t + \tau) D(t) \rangle$. Furthermore, λ can be related to γ_d so that we can write for the signal to noise ratio

$$\frac{S_O(\omega)}{S_{\text{noise}}} = 1 + 2\gamma_d S_n(\omega) \quad (13)$$

where it is assumed that the real part of the O - D correlator vanishes (which is the most favorable case for a measurement). Here $S_n(\omega)$ is the charge number fluctuation spectrum evaluated as

$$S_n(\omega) = \frac{1}{2} \lim_{t \rightarrow \infty} \int_{-\infty}^{+\infty} \left\langle \left\{ \hat{n}(t + \tau), \hat{n}(t) \right\} \right\rangle e^{i\omega\tau} d\tau \quad (14)$$

where the time evolution is obtained from a modified master equation including the back-action. Note that here we use the symmetric correlation function since the island charge itself is coupled to the quasi-particle bath, so that the detector can also receive energy from the system.

As shown in Fig. (3), the spectrum displays a resonance peak at the Josephson frequency which is broadened by the quasi-particle rate Γ (the peak is only visible in the weak dephasing regime, otherwise it is completely washed out independently of the value of γ_d). As the back-action rate γ_d increases, a maximum develops at zero frequency, which finally hides the resonance structure. This enhanced zero frequency noise results from incoherent transition induced by the detector coupling.

Near the maximum at $\omega \simeq E_J$, and for $\Gamma, \gamma_d \ll E_J$, the spectrum takes the approximate form

$$S_n(\omega) \simeq \frac{8}{3} E_J^2 \frac{(\Gamma + 2\gamma_d)}{4E_J^2(\Gamma + 2\gamma_d)^2 + (\omega^2 - E_J^2)^2}. \quad (15)$$

IV. COUNTING STATISTICS FOR THE TRANSMITTED CHARGE

We turn now to a description of the statistical distribution of the number of charges transmitted through the system during a period τ ²⁸. Specifically, we will examine the probability $P_t(N, \tau)$ that N electrons have been transferred across the right junction during the interval $[t, t + \tau]$. We note that

$$P_t(N, \tau) = \sum_{n_R} p(N + n_R, t + \tau; n_R, t), \quad (16)$$

where $p(n_R + N, t + \tau; n_R, t)$ is the joint probability that n_R electrons have passed across the right junction up to the time t and $n_R + N$ electrons up to time $t + \tau$. To obtain $P_t(N, \tau)$, we define a characteristic matrix

$$G_t(\theta, \tau) = \sum_{n_R, N} \exp(-i\theta N) \text{Tr}_{\text{qp}} \langle n_R + N | e^{-iH_{\text{tot}}\tau} | n_R \rangle \langle n_R | \rho_{\text{tot}} e^{+iH_{\text{tot}}\tau} | n_R + N \rangle, \quad (17)$$

defined so that $\text{Tr} G_t(\theta, \tau) \equiv \langle e^{i\theta N} \rangle$ is the characteristic function for $P_t(N, \tau)$. Namely,

$$P_t(N, \tau) = \int_{-\pi}^{\pi} \frac{d\theta}{2\pi} e^{+i\theta N} \text{Tr} G_t(\theta, \tau), \quad (18)$$

where the trace is taken over the states $|n\rangle$. Following the same procedure that led to Eq. (7), one can show that $G_t(\theta, \tau)$ satisfies the following master equation:

$$\partial_\tau G_t = -i [H_0, G_t] + \frac{1}{2} \sum_{n=1,2} \Gamma_n [2e^{i\theta} L_n G_t L_n^\dagger - G_t L_n^\dagger L_n - L_n^\dagger L_n G_t] \quad (19)$$

with the initial condition $G_t(\theta, 0) = \sum_{n_R} \langle n_R | \rho(t) | n_R \rangle$.

Here we will consider two limiting cases for the solution, the strong and the weak dephasing limit (see the discussion at the end of Section II). We find that in the strong dephasing case ($\Gamma \gg E_J$ or $\varepsilon \gg E_J$)

$$\text{Tr} G_t(\theta, \tau) \simeq [\sigma_{00}(t) + z\sigma_{11}(t) + z^2\sigma_{22}(t)] \exp\left[-\frac{\Gamma_r \tau}{2}(1 - z^2)\right] \quad (20)$$

while in the weak dephasing limit at resonance ($\Gamma \ll E_J, \varepsilon = 0$)

$$\begin{aligned} \text{Tr} G_t(\theta, \tau) = & \left\{ \left[\cosh \frac{\Gamma \tau f(z)}{4} + \frac{1 + 2\sigma_{11}(t) + 2z[1 - \sigma_{11}(t)]}{f(z)} \sinh \frac{\Gamma \tau f(z)}{4} \right] \right. \\ & + \frac{\Gamma}{E_J} (1 - z) \text{Im} \sigma_{02}(t) \left[\cosh \frac{\Gamma \tau f(z)}{4} + \frac{4z + 1}{f(z)} \sinh \frac{\Gamma \tau f(z)}{4} \right] \left. \right\} \exp\left(-\frac{3\Gamma \tau}{4}\right) \\ & - \frac{\Gamma}{E_J} (1 - z) \left\{ \text{Im} \sigma_{02}(t) \cos(E_J \tau) - \frac{1}{2} [\sigma_{00}(t) - \sigma_{22}(t)] \sin(E_J \tau) \right\} \exp\left(-\frac{\Gamma \tau}{2}\right), \quad (21) \end{aligned}$$

where $z = e^{i\theta}$, and $f(z) = \sqrt{1 + 8z^2}$. In Figs. 4 and 5, the resulting statistics are shown for the weak and strong dephasing cases, respectively, in the transient state (i.e. $t \simeq 0$).

As seen in Eqs. (20) and (21), $G_t(\theta, \tau)$ and hence $P_t(N, \tau)$ depend on the charge state of the island at time t . This point is further illustrated in Fig. 6 where the counting statistics at short time is shown in the strong

dephasing limit for various starting conditions $\sigma(t)$. In the limit of strong dephasing, the counting statistics depends sensitively on the initial state $\sigma(t)$. This has been exploited in Ref. 22, where the measurement of the quantum state is performed with the system taken far from degeneracy. On the contrary, the dependence on the initial condition is quickly lost in the weak dephasing regime, since the strong Josephson energy can rapidly produce a

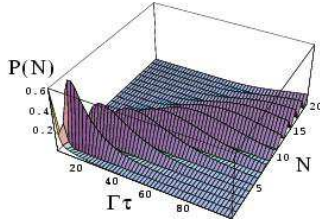


FIG. 4: $P_{t=0}(N, \tau)$ obtained by numerically solving equation (19), in the case of $\Gamma_r = 0.1\Gamma$, with initial condition $\rho_{00}(0) = 1, \rho_{22}(0) = 0$.

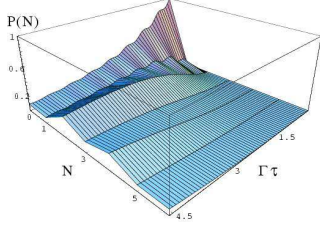


FIG. 5: The short time probability for the first few tunneling events in the weak dephasing regime ($\Gamma = 0.1E_j$) and at resonance ($\varepsilon = 0$). In this regime, the counting probability does not depend on the initial condition for ρ

change in the state, before quasi-particles have any time to be produced.

Another important limit to consider is the stationary state ($t \rightarrow \infty$), where physical properties do not depend on the initial preparation of the system. In the strong dephasing limit, Eq. (20) is reduced to the simple form

$$\text{Tr } G_\infty(\theta, \tau) \simeq \exp \left[-\frac{1}{2} \Gamma_r \tau (1 - z^2) \right]. \quad (22)$$

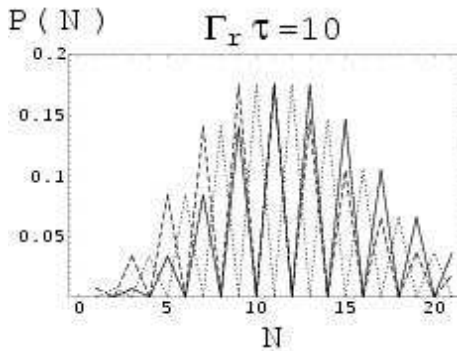


FIG. 6: Comparison among transient-state counting statistics $P_{t=0}(N, \tau)$ at $\Gamma_r \tau = 10$ in the strong dephasing regime with $\Gamma_r/\Gamma = 0.1$ for the three initial conditions a) $\sigma_{00} = 1, \sigma_{11} = \sigma_{22} = 0$ (dashed line), b) $\sigma_{11} = 1, \sigma_{00} = \sigma_{22} = 0$ (dotted line) c) $\sigma_{22} = 1, \sigma_{00} = \sigma_{11} = 0$ (continuous line).

It gives the probability distribution function for the transmitted charges

$$P_\infty(2N + 1, \tau) = 0 \quad (23a)$$

$$P_\infty(2N, \tau) = \frac{(\Gamma_r \tau / 2)^N}{N!} \exp \left(-\frac{\Gamma_r \tau}{2} \right). \quad (23b)$$

$P_\infty(N)$ shows a strong even-odd asymmetry: for even N , the distribution is Poissonian, but the probability that an odd number of electrons has passed is negligible. Below we will see that this strong parity effect manifests itself as an enhancement of zero-frequency shot noise. We leave the physical interpretation of the parity effect until we discuss shot noise in Section V.

In the weak dephasing limit, Eq. (21) is reduced to

$$\begin{aligned} \text{Tr } G_\infty(\theta, \tau) &= \exp \left(-\frac{3\Gamma\tau}{4} \right) \\ &\times \left[\cosh \frac{\Gamma\tau f(z)}{4} + \frac{1+8z}{3f(z)} \sinh \frac{\Gamma\tau f(z)}{4} \right] \end{aligned} \quad (24)$$

so that

$$P_\infty(2N, \tau) = \exp \left(-\frac{3\Gamma\tau}{4} \right) \left(\frac{1}{3} + \frac{4}{\Gamma} \frac{\partial}{\partial \tau} \right) F_N(\tau), \quad (25a)$$

$$P_\infty(2N - 1, \tau) = \frac{8}{3} \exp \left(-\frac{3\Gamma\tau}{4} \right) F_N(\tau), \quad (25b)$$

where

$$F_n(\tau) = \frac{1}{2\pi i} \oint_{|z|=1} \frac{dz}{z^{n+1}} \frac{1}{f(z)} \sinh \frac{\Gamma\tau f(z)}{4}. \quad (26)$$

This distribution function shows a much weaker (but still finite) even-odd asymmetry than the previous case [cf. Eq. (23)]. Furthermore, the distribution clearly deviates from a Poissonian function, indicating that the presence of the strong coherent tunneling of Cooper pairs tends to correlate the quasi-particle tunneling events across the right junction. This is further reflected in the deviations of the current noise from the classical shot noise value (see discussions in Section V).

One may expect that for a long waiting time ($\Gamma\tau \rightarrow \infty$), implying very large numbers of tunneled charges, the distribution of N should approach a Gaussian. In particular, this becomes an exact result if the distribution is Poissonian. In our case, on the other hand, we have

$$P_\infty(2N, \tau \rightarrow \infty) \approx \frac{5}{9} P_G(N, \tau), \quad (27a)$$

$$P_\infty(2N - 1, \tau \rightarrow \infty) \approx \frac{4}{9} P_G(N, \tau), \quad (27b)$$

where P_G is a Gaussian distribution,

$$P_G(N, \tau) = \frac{1}{\sqrt{2\pi\eta\tau}} \exp \left[-\frac{(N - I\tau/2e)^2}{2\eta\tau} \right] \quad (28)$$

with $\eta = 20/27$. The distributions for both even and odd N are separately Gaussian, but $P_\infty(N, \tau \gg \Gamma^{-1})$ as

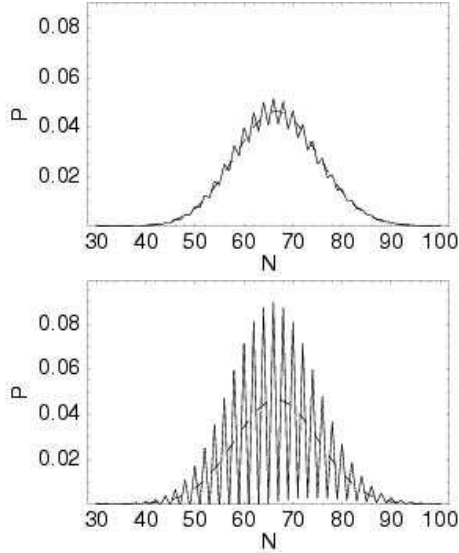


FIG. 7: Stationary-state distribution $P_\infty(N, \tau)$ at $\Gamma\tau = 100$ (a) $\Gamma_1 = \Gamma_2 = \Gamma = 10^{-5}E_J$ and (b) $\Gamma_1 = \Gamma_2 = \Gamma = 30E_J$. For a comparison, a normal distribution function given in Eq. (28) is also shown (dashed line).

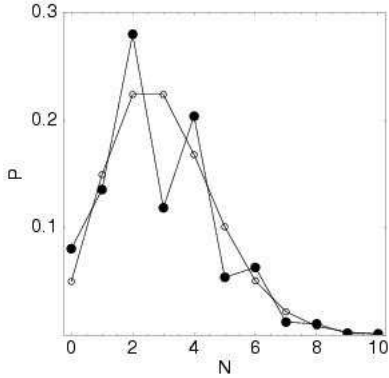


FIG. 8: Counting probability $P_\infty(N, \tau)$ at $\Gamma\tau = 4$ for $\Gamma = \sqrt{2}E_J$ (filled circle). For a comparison, the Poissonian distribution is also plotted (empty circle).

a whole is not, since even-odd asymmetry is still present. In Fig. 7 we compare the stationary-state results for $P_\infty(N, \tau)$ in the weak and strong dephasing limits with the Gaussian distribution.

Finally, it is interesting to understand what happens to the stationary counting probability $P_\infty(N, \tau)$ in the intermediate regime, i.e., when the dephasing rate is comparable to the Josephson energy. Unfortunately, an analytic expression is not available in this case; the numerical results, however, are shown in Fig. 8, where one can see that the distribution function deviates significantly from a Poissonian, being suppressed (enhanced) for odd (even) N .

V. SHOT NOISE

A deeper insight into the transport process can be obtained in the frequency domain, from a careful analysis

of the spectral power of current fluctuations. The zero-frequency shot noise could be directly determined by the second moment of the counting probability Eq. (18), see Ref. 2. Here, however, we follow a different route which allows us to get the entire current spectrum. To this end, we define the noise spectrum as

$$S(\omega) = \lim_{t \rightarrow \infty} \int_{-\infty}^{\infty} d\tau e^{i\omega\tau} \langle \{\delta I(t + \tau), \delta I(t)\} \rangle, \quad (29)$$

where $\delta I(t) = I(t) - \langle I(t) \rangle$ and $\{A, B\} = AB + BA$. The total current $I(t)$ through the system is related to the tunneling currents $I_{L/R} = -e\partial_t n_{L/R}$ across each junction by¹³

$$I(t) = \frac{C_L}{C_\Sigma} I_R(t) - \frac{C_R}{C_\Sigma} I_L(t). \quad (30)$$

To simplify the evaluation of $S(\omega)$, it is convenient to introduce the spectral densities of currents flowing across the individual junctions and the cross correlation spectral powers. Therefore, in a way analogous to Eq. (29), we write ($i, j = L, R$)

$$S_{ij}(\omega) = \lim_{t \rightarrow \infty} \int_{-\infty}^{\infty} d\tau e^{i\omega\tau} \langle \{\delta I_i(t + \tau), \delta I_j(t)\} \rangle, \quad (31)$$

which allows to express the total shot noise spectrum in the form

$$S(\omega) = \frac{C_R^2}{C_\Sigma^2} S_{LL}(\omega) + \frac{C_L^2}{C_\Sigma^2} S_{RR}(\omega) - \frac{C_L C_R}{C_\Sigma^2} [S_{LR}(\omega) + S_{RL}(\omega)]. \quad (32)$$

In the stationary state $\langle I \rangle = \langle I_L \rangle = -\langle I_R \rangle$, so that $S(\omega) = S_{LL}(\omega) = S_{RR}(\omega)$ in the zero-frequency limit. In the opposite limit ($\omega \rightarrow \infty$), $S(\omega) = (C_L^2/C_\Sigma^2)S_{RR}(\omega) = (C_L^2/C_\Sigma^2)2e\langle I \rangle$ ^{3,4,13}. In our case, the left junction is (nearly) at resonance for the Cooper pair tunneling and therefore $\lim_{\omega \rightarrow \infty} S_{LL}(\omega) = 0$.

In order to obtain $S_{ij}(\omega)$ we have to calculate two-time correlation functions. We follow the standard procedure based on the quantum regression theorem²⁶ and define the auxiliary matrices

$$\chi^{(j)}(t, \tau) = \text{Tr}_{\text{qp}} \{ e^{-iH\tau} n_j \rho_{\text{tot}}(t) e^{iH\tau} \}, \quad (33a)$$

$$\eta^{(j)}(t, \tau) = \text{Tr}_{\text{qp}} \{ e^{-iH\tau} \rho_{\text{tot}}(t) n_j e^{iH\tau} \}, \quad (33b)$$

where the index j runs over the left and right junctions ($j = L, R$). These auxiliary operators, $\chi^{(j)}$ and $\eta^{(j)}$, satisfy a master equation of exactly the same form as Eq. (7) (but with respect to τ instead of t and, of course, with different initial conditions). Their relevance can be understood by noticing that the correlation functions can be expressed directly in terms of their average values²⁹:

$$\begin{aligned} \langle \{\delta I_R(t + \tau), \delta I_R(t)\} \rangle &= e^2 (\partial_\tau - \partial_t) \sum_{n_R} \sum_{n=1,2} \Gamma_n \langle n, n_R | \chi^{(R)}(t, \tau) + \eta^{(R)}(t, \tau) | n, n_R \rangle \\ &\quad - 2 \langle I_R(t) \rangle^2 - 2e \langle I_R(t) \rangle \delta(\tau), \end{aligned} \quad (34)$$

$$\langle \{\delta I_L(t + \tau), \delta I_L(t)\} \rangle = 2e^2 (\partial_t - \partial_\tau) (\partial_\tau + \Gamma) \sum_{n_R} \langle 2, n_R | \chi^{(L)}(t, \tau) + \eta^{(L)}(t, \tau) | 2, n_R \rangle - 2 \langle I_L(t) \rangle^2 \quad (35)$$

and

$$\begin{aligned} \langle \{\delta I_L(t + \tau), \delta I_R(t)\} \rangle + \langle \{\delta I_R(t + \tau), \delta I_L(t)\} \rangle &= e^2 (\partial_t - \partial_\tau) \sum_{n_R} \left\{ 2(\partial_\tau + \Gamma) \langle 2, n_R | \chi^{(R)} + \eta^{(R)} \right. \\ &\quad \left. | 2, n_R \rangle - \sum_{n=1,2} \Gamma \langle n, n_R | \chi^{(L)} + \eta^{(L)} | n, n_R \rangle \right\} - 4 \langle I_L(t) \rangle \langle I_R(t) \rangle. \end{aligned} \quad (36)$$

The problem is now reduced to (a) solving a master equations of the form given in Eq. (7) to get $\rho(t)$, $\chi^{(j)}(t, \tau)$, and $\eta^{(j)}(t, \tau)$ for respective initial conditions, and (b) evaluating Eqs. (34), (35), and (36) to obtain the correlation functions. Following this procedure and performing the Fourier transforms of the resulting correlation functions, we find that in the stationary state

$$\frac{S_{RR}(\omega)}{2e \langle I \rangle} = 1 - \langle A | \frac{\Gamma(M - 2\Gamma)}{\omega^2 + M^2} | A \rangle, \quad (37)$$

$$\frac{S_{LL}(\omega)}{2e \langle I \rangle} = 2 \langle B | \frac{M - \Gamma}{\omega^2 + M^2} (M | C \rangle - 2\Gamma | A \rangle), \quad (38)$$

and

$$\frac{S_{LR}(\omega) + S_{RL}(\omega)}{2e \langle I \rangle} = 2 \langle B | \frac{(M - \Gamma)(M - 2\Gamma)}{\omega^2 + M^2} | A \rangle + \langle A | \frac{\Gamma}{\omega^2 + M^2} (M | C \rangle - 2\Gamma | A \rangle), \quad (39)$$

where we have used the bra-ket notations

$$M = \begin{pmatrix} \Gamma & \Gamma & iE_J/2 & -iE_J/2 \\ 0 & \Gamma & -iE_J/2 & iE_J/2 \\ iE_J/2 & -iE_J/2 & \Gamma/2 + i\varepsilon & 0 \\ -iE_J/2 & iE_J/2 & 0 & \Gamma/2 - i\varepsilon \end{pmatrix}, \quad (40)$$

$$|A\rangle = \begin{pmatrix} 1 \\ 0 \\ 0 \\ 0 \end{pmatrix}, |B\rangle = \begin{pmatrix} 0 \\ 1 \\ 0 \\ 0 \end{pmatrix}, \quad (41)$$

and

$$|C\rangle = |A\rangle + |B\rangle + \left(\frac{E_J}{\Gamma} + \frac{E_J}{\Gamma_r} \right) \begin{pmatrix} 0 \\ 0 \\ -i \\ +i \end{pmatrix}. \quad (42)$$

From Eqs. (37), (38), (39), and (32), it follows that the zero-frequency noise is given by

$$\frac{S(0)}{2e \langle I \rangle} = 2 - \frac{8E_J^2(E_J^2 + 2\Gamma^2)}{(3E_J^2 + \Gamma^2 + 4\varepsilon^2)^2}. \quad (43)$$

In the strong dephasing limit ($\Gamma \gg E_J$), the second term in Eq. (43) becomes negligibly small, as it vanishes as $(E_J/\Gamma)^2$. Therefore, the zero-frequency shot noise is enhanced approximately by a factor 2 compared with its classical value, $2e \langle I \rangle$. This can be understood in terms of the Josephson quasi-particle (JQP) cycle^{17,18,19}. Because of the fast quasi-particle tunneling across the right junction, each Cooper pair that has tunneled into the central island breaks up immediately into quasi-particles, and quickly tunnels out. The charge is therefore transferred in units of $2e$ (compared with e in classical charge transfer) for each JQP cycle. This was already confirmed in the counting statistics of the transmitted charges. According to Eq. (23), the probability that an odd number

of electrons are transferred is zero and charges are transferred only in pairs. In the weak ($\Gamma \ll E_J$) and moderate ($\Gamma \simeq E_J$) dephasing limits, the semiclassical JQP picture breaks down and we do not have shot noise enhancement any longer.

In the limit $\Gamma \ll E_J$, the period of oscillations of Cooper pair is very short compared to the typical time for quasi-particles to tunnel out of the central island. The system can be regarded as a single-junction circuit, where the quasi-particle tunneling events are independent. The Fano factor $S(0)/2e\langle I \rangle \approx 10/9$, becomes much closer to unity in this limit. The small deviation from the Poisson value is due to the fact that the quasi-particle tunneling events cannot be considered as independent because Coulomb blockade allows only one Cooper pair to oscillate coherently across the left junction. Therefore, the tunneling process corresponding to $|2\rangle \rightarrow |1\rangle$ is likely to be followed by $|1\rangle \rightarrow |0\rangle$. It is clear that this behavior is related to the residual even-odd asymmetry we found in the counting statistics, Eq. (25), even in the long waiting-time limit ($\Gamma\tau \gg 1$), Eq. (27).

With moderate dephasing ($\Gamma \simeq E_J$), quasi-particle tunneling events across the right junction are strongly affected by the *coherent* oscillation of Cooper pairs across the left junction. Indeed, this effect gives rise to the significant deviation from the Poissonian distribution of the tunneling statistics, Eq. (25). Most remarkably, it leads to a suppression of the shot noise. The strongest suppression, by a factor of $2/5$, is achieved at resonance ($\varepsilon = 0$) for $\Gamma = \sqrt{2}E_J$, see Fig. 9. This is reminiscent of the shot noise suppression in (non-superconducting) double-junction systems⁴, whose maximal suppression is by factor $1/2$ for the symmetric junctions. We emphasize, however, that in the latter case, the coherence was not essential. In our case, on the contrary, the role of coherence becomes evident by noticing that the dip in Fano factor disappears when moving away from the resonant condition as shown in Fig. 9.

B. Finite-Frequency Noise

In Figs. 10 and 11 we show the typical behavior of the finite-frequency noise spectrum in the (a) strong and (b) weak dephasing limits. It is interesting to notice that (only) in the weak dephasing limit ($\Gamma \ll E_J$), there is a resonance peak of the form

$$\frac{S(\omega)}{2eI} \approx \frac{C_R^2}{2C_\Sigma^2} \frac{E_J^2 + 2\varepsilon^2}{(\omega - \omega_0)^2 + \Gamma^2/4}, \quad (44)$$

where the resonance frequency is given by

$$\omega_0 \simeq \sqrt{E_J^2 + \varepsilon^2} \left[1 - \frac{\Gamma^2(E_J^2 + 3\varepsilon^2/2)}{4(E_J^2 + \varepsilon^2)^2} \right]. \quad (45)$$

Clearly, the peak is an effect of coherent quantum oscillations between the two energy levels separated by $\omega_0 \xrightarrow{\Gamma \rightarrow 0} \sqrt{E_J^2 + \varepsilon^2}$, induced by the Josephson effect

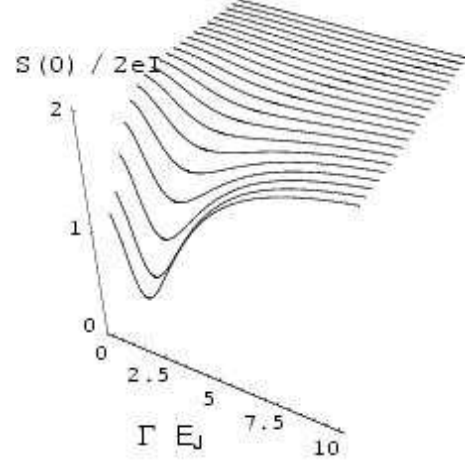


FIG. 9: Normalized zero-frequency shot noise for $\varepsilon/E_J = 0, 0.25, \dots, 5$. The dip in the noise is most pronounced at resonance ($\varepsilon = 0$).

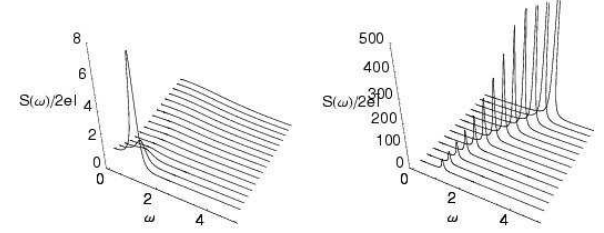


FIG. 10: Current noise power, (a) at resonance ($\varepsilon = 0$) for $\Gamma/E_J = 0, 0.25, \dots, 5$, and (b) at a fixed weak dephasing rate ($\Gamma = 0.1E_J$) for $\varepsilon/E_J = 0, 0.25, \dots, 5$.

across the left junction. As expected, the resonance peak is reduced in its height and broadened in its width with increasing Γ . On the contrary, as ε increases, the peak gets sharper and the peak height increases quadratically with ε . However, this should not be confused with the zero-frequency case, where ε effectively enhances the decoherence effects. As ε increases, the Josephson oscillation across the left junction becomes faster, and there are

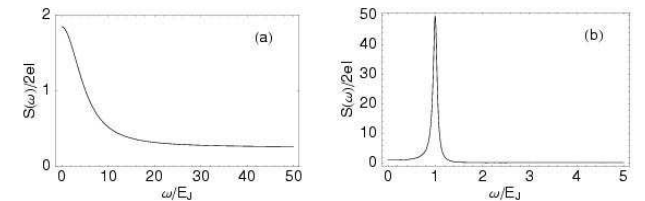


FIG. 11: Typical behavior of noise power spectrum $S(\omega)$ as a function of frequency ω in the (a) strong ($\Gamma_{1,2} \gg E_J$) and (b) weak ($\Gamma_{1,2} \ll E_J$) quasi-particle tunneling limits. For both plots, $\varepsilon = 0$ and $C_L = C_R = C_\Sigma/2$ were assumed.

less chances that it is interrupted by the quasi-particle tunneling across the right junction. This, in turns, implies that the coherent oscillation is better defined and the spectral component (especially $S_{LL}(\omega)$) at frequency ω_0 is highly enhanced. For a vanishingly small quasi-particle tunneling rate, $S_{LL}(\omega)/2eI$ would approximately become a delta-like function, centered at $\omega = \sqrt{E_J^2 + \varepsilon^2}$. However, one should not be misled by this result, since the noise is always proportional to the average current, which vanishes in this limit.

It is worth mentioning here on the relation between this result and the description of the noise output from linear detector¹⁰. In the setup considered in this work, the right electrode has the role of the detector of Cooper pair oscillations; since the total current in the circuit is due to quasi-particle tunneling (i.e. it is a *dissipative* current), the output signal may be considered as classical. This has to be compared to the case of a detector measuring the charge on the island. There, the back-action of the detector was essential to produce an observable result. In the case of the current, instead, the "detector" is intrinsically part of the system and it couples to the observed quantity in an essentially non-linear way.

VI. CONCLUSIONS

In this paper we considered properties of the distribution of the transmitted charge in a superconducting SET tuned close to a Cooper pair resonance. The dominant process to the transport in the regime considered here, is the JQP cycle, a process in which coherent Cooper pair oscillations are accompanied by (incoherent) quasi-particle tunneling. The interplay between the coherence and the strong Coulomb blockade manifests itself in various ways both in the counting statistics and in the shot noise. We found two distinct regimes characterized by

different ratios of the time scales for dephasing and relaxation, $\tau_r \ll \tau_\varphi$ in the strong dephasing limit or $\tau_r \sim \tau_\varphi$ in the opposite case of weak dephasing.

A generic feature of the counting statistics, valid in both the regimes, is its even-odd asymmetry related to the fact that charge transport is mediated by the Cooper pair tunneling. Other properties are more pronounced in one of the two regimes. An example is the dependence of $P_t(N, \tau)$ on the initial time t . This is clearly visible in the strong dephasing limit while quickly lost in the weak dephasing regime since, because of the strong Josephson energy, the state changes significantly before quasi-particles have any time to be produced. Another important point is that the counting statistics is not Poissonian, due to the relevance of correlations between different tunneling events. As a consequence the Fano factor is different from the classical value. The maximal suppression of the zero-frequency shot noise is observed when the quasi-particle tunneling rate is comparable to the frequency scale of the coherent Cooper pair oscillations.

We finally investigated the shot noise at finite frequencies, which shows a resonance peak at the Josephson oscillation frequency. This maximum can be interpreted as an effect of coherent quantum transitions between the two energy levels involved in the transport phenomena in the device.

Acknowledgments

We thank D.V. Averin, Y. Blanter, and J. Siewert for very useful discussions. We acknowledge financial support from European Community (IST-FET-SQUBIT) and INFM (PAIS-TIN). M.-S.C. acknowledges the support from the Swiss-Korean Outstanding Research Efforts Award program.

¹ M. J. M. de Jong and C. W. J. Beenakker, in *Mesoscopic Electron Transport*, edited by L. L. Sohn, L. P. Kouwenhoven, and G. Schön (Kluwer Academic Publishers, Dordrecht, 1997).
² Y. M. Blanter and M. Büttiker, Phys. Rep. **336**, 1 (2000).
³ J. H. Davies *et al.*, Phys. Rev. B **46**, 9620 (1992).
⁴ S. Hershfield *et al.*, Phys. Rev. B **47**, 1967 (1993).
⁵ G. Schön and A.D. Zaikin, Phys. Rep. **198**, 237 (1990).
⁶ D.V. Averin and K.K. Likharev, *Mesoscopic Phenomena in Solids*, B.L. Altshuler, P.A. Lee, and R.A. Webb Eds., (North-Holland, Amsterdam, 1991).
⁷ R. J. Schoelkopf *et al.*, Science **280**, 1238 (1998); A. N. Korotkov, Appl. Phys. Lett. **69**, 2593 (1996).
⁸ Yu. Makhlin, G. Schön, and A. Shnirman, Phys. Rev. Lett. **85**, 4578 (2000).
⁹ M. H. Devoret and R. J. Schoelkopf, Nature **406**, 1039 (2000).
¹⁰ D. V. Averin, in "Exploring the Quantum-Classical Frontier: Recent Advances in Macroscopic and Mesoscopic

Quantum Phenomena", Eds. J. R. Friedman and S. Han, to be published (cond-mat/0004364); D. V. Averin, preprint (2002), cond-mat/0202082.
¹¹ A. Aassime, G. Johansson, G. Wendin, R. J. Schoelkopf, and P. Delsing, Phys. Rev. Lett. **86**, 3376 (2001); G. Johansson, A. Käck, and G. Wendin, Phys. Rev. Lett. **88**, 046802 (2002).
¹² U. Hanke, Y. M. Galperin, K. A. Chao, and N. Zou, Phys. Rev. B **48**, 17209 (1993); U. Hanke, Y. M. Galperin, and K. A. Chao, *ibid.* **50**, 1595 (1994).
¹³ A. N. Korotkov, Phys. Rev. B **49**, 10 381 (1994).
¹⁴ E. V. Sukhorukov, G. Burkard, D. Loss, cond-mat/0010458.
¹⁵ D. V. Averin, cond-mat/0010052.
¹⁶ D. Loss and E.V. Sukhorukov, Phys. Rev. Lett. **84**, 1035 (2000); M.-S. Choi, C. Bruder, and D. Loss, Phys. Rev. B **62**, 13 569 (2000); F. Plastina, R. Fazio, and G. M. Palma, Phys. Rev. B **64**, 113306 (2001).
¹⁷ T. A. Fulton *et al.*, Phys. Rev. Lett. **63**, 1307 (1989).

¹⁸ D. V. Averin and V. Y. Aleshkin, Pis'ma Zh. Eksp. Teor. Fiz. **50**, 331 (1989) [JETP Lett. **50** (7), 367 (1989)].

¹⁹ A. Maassen van den Brink, G. Schön, and L. J. Geerligs, Phys. Rev. Lett. **67**, 3030 (1991).

²⁰ D. V. Averin and H. T. Imam, Phys. Rev. Lett. **76**, 3814 (1996).

²¹ A. A. Clerk, S. M. Girvin, A. K. Nguyen, and A. D. Stone, preprint (2002), cond-mat/0203338.

²² Y. Nakamura, Y. A. Pashkin, and J. S. Tsai, Nature **398**, 786 (1999).

²³ M.-S. Choi, F. Plastina, and R. Fazio, Phys. Rev. Lett. **87**, 116 601 (2001).

²⁴ A microscopic derivation is given in G.-L. Ingold and Y. V. Nazarov, in *Single Charge Tunneling: Coulomb Blockade Phenomena in Nanostructures*, edited by H. Grabert and M. Devoret (Plenum Press, New York, 1992).

²⁵ N. R. Werthamer, Phys. Rev. **147**, 255 (1966); A. I. Larkin and Y. N. Ovchinnikov, Zh. Eksp. Teor. Fiz. **51**, 1535 (1966) [Sov. Phys. -JETP **24**, 1035 (1967)].

²⁶ H. J. Carmichael, *An Open Systems Approach to Quantum Optics* (Springer-Verlag, Berlin, 1993); K. Blum, *Density Matrix Theory and Applications*, 2 ed. (Plenum Press, New York, 1996).

²⁷ M.-S. Choi *et al.*, Europhys. Lett. **53**, 251 (2001).

²⁸ L. S. Levitov and G. B. Lesovik, JETP Lett. **58**, 230 (1993); L. S. Levitov, H.-W. Lee, and G. B. Lesovik, J. Math. Phys. (N.Y.) **37**, 10 (1996).

²⁹ The last term in each of Eqs. (34)-(36) describes the auto-correlation of single current spikes and arises because the tunneling events are considered to be instantaneous, see Refs. 3,4,13.

³⁰ A. N. Korotkov, Phys. Rev. B. **60**, 5737 (1999); A. N. Korotkov and D. V. Averin, cond-mat/0002203.